IL NUOVO CIMENTO **38 C** (2015) 147
DOI 10.1393/ncc/i2015-15147-5

COLLOQUIA: LaThuile15

Search for pair production of vector-like partners of the top quark (T), with T → tH, H → $\gamma\gamma$

G. FASANELLA on behalf of the CMS COLLABORATION

ULB - Université Libre de Bruxelles Bruxelles, Belgium and
Università Sapienza di Roma - Roma, Italy

received 2 October 2015

Summary. — We present a search for a heavy vector-like quark with charge 2/3 (top partner, T). We search for events where the top partner is produced in pairs and where at least one of them decays into a top quark and a Higgs boson. We focus on the decays of the Higgs boson to photons to allow for full mass reconstruction. The observed data are in agreement with the standard model prediction. We proceed to set observed (expected) 95% confidence level upper limits on the production cross section of strong $T\bar{T}$ production, excluding the existence of top quark partners with mass up to 540 (607) GeV using 19.7 fb^{-1} of integrated luminosity.

PACS `14.80.Bn` – Standard Model Higgs Boson.
PACS `14.65.Ha` – Top quarks.
PACS `14.70.Bh` – Photons.

1. – Introduction

The recent discovery of a Higgs boson at the LHC [1, 2] sets strong constraints on a simple, sequential fourth generation of quarks. Still, the presence of new physics is necessary to stabilize the mass of the Higgs boson, if one wants to avoid an unnaturally high level of fine tuning of the theory. In supersymmetry bosonic top quark partners would cancel the loops that induce this large instability. Similarly, fermionic partner quarks to the third generation quarks can also serve this purpose [3].

In this note, we describe the analysis and the results of [4], presenting a search for a new T particle, which is a vector-like partner of the top quark. The left- and right-handed chiral states of vector-like fermions transform in the same fashion under the $SU(2)$ gauge transformations of the weak interactions. Several theories such as Little Higgs [5] and Composite Higgs [6] predict such particles, with masses typically at or below the TeV range. Top quark partners can be produced in pairs through strong interactions, or singly through electroweak interactions. The cross section is typically larger for pair production up to T quark masses in the 600–800 GeV range, although the exact crossing point depends on the details of the weak interactions of these exotic objects [7]. We focus here on the T quark pair production.

Older searches for heavy vector-like quarks focused separately either on the T $\rightarrow$ bW or T $\rightarrow$ tZ final states [8,9]. The precise knowledge of the Higgs boson mass now allows us to target the T $\rightarrow$ tH decay as well.

2. – Experimental setup

This measurement uses data from proton-proton collisions, produced at a center-of-mass energy of 8 TeV, corresponding to an integrated luminosity of $L = 19.7\ \text{fb}^{-1}$ [10]. The data were collected by the CMS detector at the Large Hadron Collider (LHC) in 2012. The data have been recorded by requiring two photons with large momentum transverse to the beam axis, p_{T}, in the online selection performed by the trigger system, similarly to the H $\rightarrow \gamma\gamma$ analysis [11].

A detailed description of the CMS detector can be found elsewhere [12]. Its central feature is a 3.8 T superconducting solenoid of 6 m internal diameter. Within its field volume there are the silicon tracker, the crystal electromagnetic calorimeter (ECAL), and the brass/scintillator sampling hadron calorimeter (HCAL). The muon system, composed of drift tubes, cathode strip chambers and resistive-plate chambers, is installed outside the solenoid, embedded in the steel return yoke. CMS uses a right-handed coordinate system, with the origin at the nominal interaction point, the x-axis pointing to the center of the LHC, the y-axis pointing up (perpendicular to the LHC plane), and the z-axis along the counterclockwise-beam direction. The polar angle θ is measured from the positive z-axis and the azimuthal angle ϕ is measured in the x-y plane. The pseudorapidity η is defined as $-\ln[\tan(\theta/2)]$.

The photon reconstruction and identification criteria are the same used by the cut-based H $\rightarrow \gamma\gamma$ analysis [11]. Jets are reconstructed with the fastjet software version 3.0.4 [13], using PF candidates as inputs and clustered with the anti-k_{T} [14] algorithm using a distance parameter $R = 0.5$. More details about jet selection and the cuts used can be found in [15]. To identify jets originating from the hadronization of bottom quarks, the Combined Secondary Vertex (CSV) b-tagging algorithm [16] is employed. Muons are measured [17] with the combination of the tracker and the muon system, in the pseudorapidity range $|\eta| < 2.4$. Electrons are detected [18] as tracks in the tracker pointing to energy clusters in ECAL in the range $|\eta| < 2.5$. The full details of the electron and muon identification criteria are described elsewhere [11].

3. – Analysis strategy

This analysis searches for events in which two heavy top quark partners are produced and at least one of them decays to a top quark and a Higgs boson, which in turn decays to two photons. The main advantage of this decay channel is that we can precisely measure the mass of the diphoton system ($m_{\gamma\gamma}$) and search for a narrow resonance in the diphoton invariant mass distribution centered around the Higgs boson mass ($\approx$ 125 GeV), estimating the background directly from data sidebands. The analysis selects events in which two isolated photons are present in addition to further leptons and jets coming from the decay of the other top and Higgs particles present in the final state.

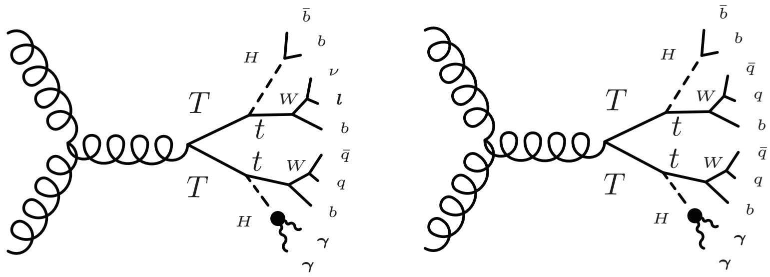

Fig. 1. – Example Feynman diagrams for top quark partners production and decay in the hadronic (left) and leptonic (right) channels.

Two search channels are defined, targeting different decay modes of the top quark partners:

- the *leptonic channel* searches for events with a pair of photons and at least one isolated high-p_T electron or muon. This channel targets events where at least one charged lepton appears either in the top quark decay chain, or in the decay chain stemming from the second top quark partner. A Feynman diagram representing one such example is depicted in the right side of fig. 1.

- the *hadronic channel* searches for events with a pair of photons and no isolated electrons or muons. This channel targets events in which a top quark partner decay chain leads only to quarks, and the top plus Higgs boson, coming from the other top partner, decays hadronically. An example diagram is given in the left side of fig. 1;

Events with two prompt photons arise from direct QCD production as well as emission in top quark production ($\gamma\gamma$+jets, $\mathrm{t\bar{t}}+\gamma\gamma$, $\mathrm{t}+\gamma\gamma$). Jets in $\mathrm{t\bar{t}}$ events can also be misreconstructed as photons due to the high number of jets in the final state. Monte Carlo modeling of these backgrounds is not reliable in the kinematic regions used for this analysis (high number of jets in the final state). We derive a control sample from data to optimize the selection, and we use data from $m_{\gamma\gamma}$ sidebands to estimate the non-resonant background for the statistical analysis. The resonant contribution to the background due to $\mathrm{t\bar{t}H}$ is estimated from MC.

Simulated samples are used to estimate the yield of $\mathrm{T\bar{T}}$ production. Signal samples with varying top quark partner mass and decay modes have been obtained through MadGraph version 5 [19] for the hard scatter and Pythia version 6.4 [20] for parton shower/hadronization and underlying event modeling. The cross sections for $\mathrm{T\bar{T}}$ production have been computed at next-to-next-to-leading order (NNLO) + next-to-next-to-leading logarithm (NNLL) soft gluon resummation using the Top++2.0 computer program [21], and MSTW2008nnlo68cl parton density functions (PDFs) [22]. Additional details can be found elsewhere [4].

4. – Event selection

The main aim of the event selection optimization is to discriminate the $\mathrm{T\bar{T}}$ signal from the reducible background contributions, which are non resonant in $m_{\gamma\gamma}$ ($\gamma\gamma$+jets, top processes). An optimization of the cuts is performed using a data-driven control

TABLE I. – *Final selection for hadronic and leptonic channel.*

Variable	Hadronic channel	Leptonic channel
$p_{\mathrm{T}}(\gamma_1)$	$> \frac{3}{4} m_{\gamma\gamma}$ GeV	$> \frac{1}{2} m_{\gamma\gamma}$ GeV
$p_{\mathrm{T}}(\gamma_2)$	35 GeV	25 GeV
$\mathrm{n_{jets}}$	≥ 2	≥ 2
H_{T}	≥ 1000 GeV	≥ 770 GeV
leptons	0	≥ 1
b tags	≥ 1	-

sample, for non resonant background. A control sample is obtained in data, using events containing at least one photon which passes loose identification requirements but not passing the final event selection.

The optimization is performed, separately for the leptonic and the hadronic channel, using $\mathrm{T\bar{T}}$ Monte Carlo with $m_{\mathrm{T}} = 700$ GeV as signal and the sum of the data-driven background and $\mathrm{t\bar{t}H}$ simulation as background. We perform a full optimization inspecting different kinematic variables for photons and jets and choosing the most discriminant and less correlated ones as input variables for a multivariate optimization. The signal is characterized by the presence of high p_{T} photons and high jet and b-jet multiplicity, and so by a higher H_{T} variable, defined as the sum of the transverse momenta of all the objects in the final state.

We optimize our event selection working point using, as a figure of merit, the 95% confidence level (CL) expected upper limit (UL) on $\sigma(\mathrm{T\bar{T}})$. The final selection for the two channels, corresponding to the chosen working point, is reported in table I.

The background is obtained by fitting the observed diphoton mass distributions in each event category (hadronic or leptonic) over the range $100 < m_{\gamma\gamma} < 180$ GeV. Thus the choice of the background parametrisation is a key component for the signal extraction. This choice is based upon a data-driven criterion, which starts by finding functions that fit well the observed mass distribution in the background only hypothesis. We compare the maximum potential bias on the number of fitted background events to the statistical error of the fit, and we choose the background model such that the bias is at least five times smaller than the statistical error. For both the hadronic and leptonic channel, a simple exponential is chosen.

5. – Systematic uncertainties

All simulation-derived experimental systematic uncertainties apply to signal and the $\mathrm{t\bar{t}H}$ resonant background. As explained in sect. **4**, systematics affecting the data-driven background prediction are not considered as the procedure for choosing the background parametrization ensures that they can be safely neglected, relative to the statistical error of the fit. All systematics are summarized in table II.

6. – Results

Background model unbinned maximum-likelihood fits to the diphoton mass distribution, under the hypothesis of no signal, are shown for the hadronic and leptonic channel in fig. 2, under the hypothesis $m_{\mathrm{T}} = 700$ GeV.

TABLE II. – *Summary of the adopted systematic uncertaintes.*

	$T\bar{T}$	$t\bar{t}H$
Luminosity	$\pm 2.6\%$	$\pm 2.6\%$
PDF	-	$\pm 8.1\%$
QCD scale	-	$+4/-9\ \%$
Photon Energy Resolution	$+4/-2\ \%$	$+4/-2\%$
Photon Energy Scale	$+1/-4\ \%$	$+1/-4\%$
Photon ID Efficiency	$\pm 2\%$	$\pm 2\%$
Trigger	$< 0.1\%$	$< 0.1\%$
JEC	$\pm 2\%$ (had) $\pm 1\%$ (lep)	$\pm 7\%$ (had) $\pm 5\%$ (lep)
JER	$\pm 1\%$	$< 0.5\%$
b-tagging	$< 0.5\%$ (had)	$< 0.5\%$ (had)
Pile-up identification	$\pm 2\%$	$\pm 2\%$
Lepton Reconstruction	$\pm 1\%$ (lep)	$\pm 1\%$

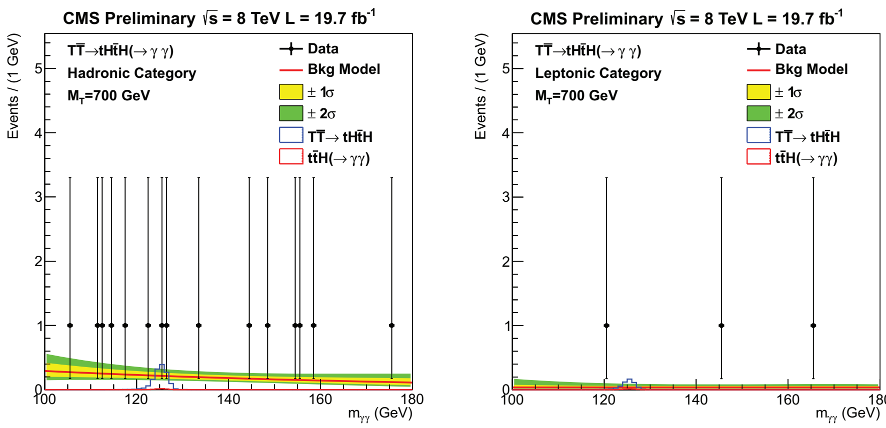

Fig. 2. – Diphoton invariant mass distribution for candidate $T\bar{T}$ events for the hadronic (left) and leptonic (right) channel. The signal is normalized to the predicted theoretical cross section corresponding to $m_{\mathrm{T}} = 700\,\mathrm{GeV}$. Background predictions coming from the fit are shown as a red line, and bands corresponding to 68% (yellow) and 95% (green) are added.

We do not observe any significant excess in the data, since observed data in the signal window are compatible with background expectations. By analyzing the invariant mass spectra of the two channels, an upper limit on the production cross section of $T\bar{T}$ quark pairs can be set. A 95% confidence level exclusion limit on the signal strength modifier is evaluated using a modified frequentist CL_s approach, taking the profile likelihood ratio as a test statistic [23-25]. The limits on the production cross section times branching ratio using the CL_s computation are shown in fig. 3, for the hadronic and leptonic channels. The expected limit is shown as a dotted black line, and the bands corresponding to 68% (yellow) and 95% (green) probability are added. The observed limit is represented by a black line. As can be seen the hadronic channel expected exclusion reaches top quark partner masses up to 538 GeV. The upper limit expected in the leptonic channel

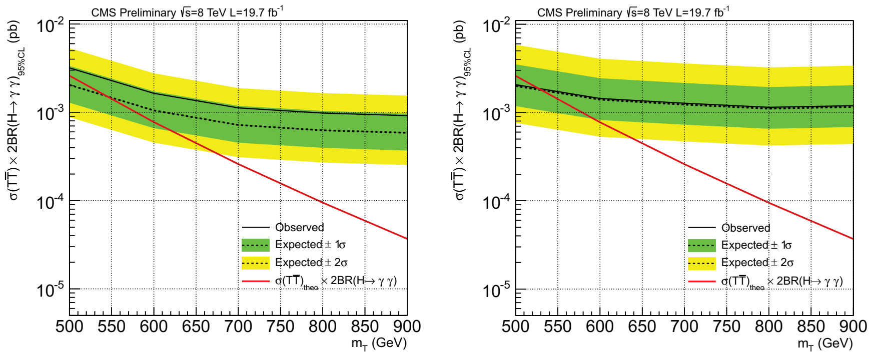

Fig. 3. – 95% C.L. upper limit on heavy vector-like partners of the top quark (T), with $\mathrm{T} \to \mathrm{tH}(\to \gamma\gamma)$, production in the hadronic (left) or leptonic (right) channel.

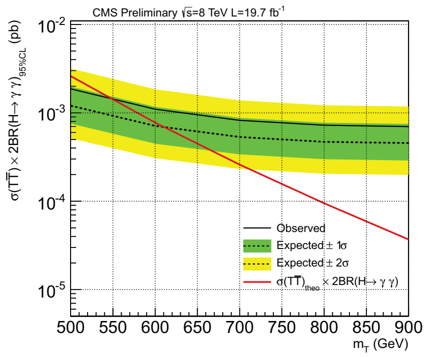

Fig. 4. – 95%C.L. upper limit on heavy vector-like partners of the top quark (T), with $\mathrm{T} \to \mathrm{tH}(\to \gamma\gamma)$, production is shown for the combination of the two channels

corresponds to an exclusion of top quark partner with masses up to 522 GeV. Combining the two channels we proceed to set 95% confidence level upper limits on the production cross section of strong $\mathrm{T\bar{T}}$ production. We thus proceed to translate the limits into observed (expected) exclusion bounds to the existence of top quark partners with masses up 540 (607) GeV using 19.7 fb^{-1} of integrated luminosity. All these results are obtained under the assumption of $\mathcal{B}(\mathrm{T} \to \mathrm{tH}) = 100\%$. The two channels are combined, and the resulting upper limit is shown in fig. 4.

Relaxing the assumption that $\mathcal{B}(\mathrm{T} \to \mathrm{tH}) = 100\%$ we can proceed to set limits as a function of $\mathcal{B}(\mathrm{T} \to \mathrm{tH})$ and m_{T}. In fig. 5 we show the expected and observed region of exclusion in the 2-dimensional space of $\mathcal{B}(\mathrm{T} \to \mathrm{tH})$ and m_{T}. As can be seen from fig. 5 our result is only sensitive to $\mathcal{B}(\mathrm{T} \to \mathrm{tH})$ and almost not sensitive to different values of $\mathcal{B}(\mathrm{T} \to \mathrm{Wb})$ and $\mathcal{B}(\mathrm{T} \to \mathrm{tZ})$.

Nevertheless, we also proceed to show the expected and observed exclusion region in the branching ratio triangle in fig. 6 for the T quark mass. Every point in the triangle corresponds to a particular set of branching fraction values subject to the constraint that all three add up to one. The branching fraction for each mode decreases from one at the corner labeled with the decay mode to zero at the opposite side of the triangle.

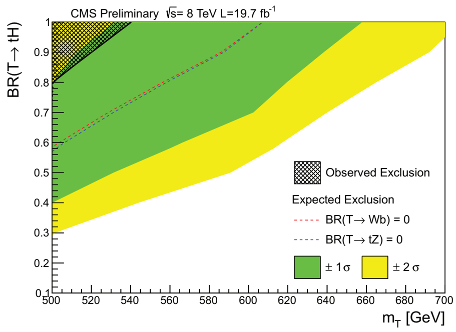

Fig. 5. – Expected and observed region of exclusion in the 2D phase space of $\mathcal{B}(\mathrm{T} \to \mathrm{tH})$ and m_{T}. Different dashed lines correspond to different assumptions on the branching ratios of the top partner: $\mathcal{B}(\mathrm{T} \to \mathrm{Wb}) = 0$ (and consequently $\mathcal{B}(\mathrm{T} \to \mathrm{tZ}) = 1 - \mathcal{B}(\mathrm{T} \to \mathrm{tH})$) in red and $\mathcal{B}(\mathrm{T} \to \mathrm{tZ}) = 0$ (and consequently $\mathcal{B}(\mathrm{T} \to \mathrm{Wb}) = 1 - \mathcal{B}(\mathrm{T} \to \mathrm{tH})$) in blue.

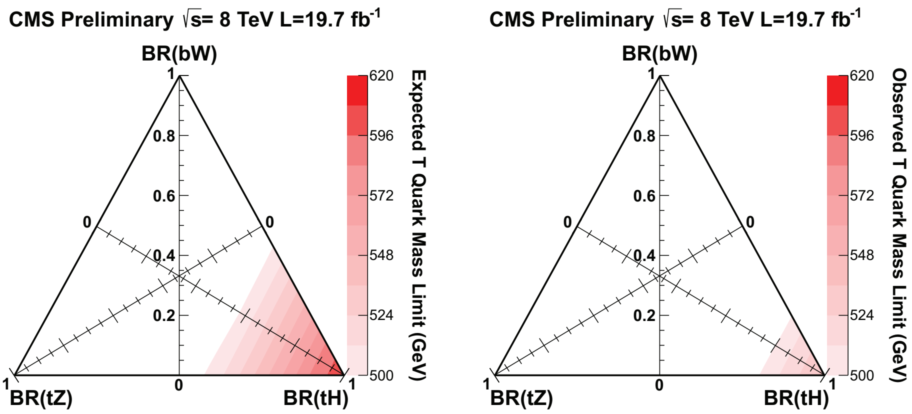

Fig. 6. – Branching fraction triangle with expected (left) and observed (right) limits for the T quark mass. We cannot exclude any T quark with a mass greater of 500 GeV in the white region of the triangle.

7. – Summary

The first search for $\mathrm{T\bar{T}}$ production in events in which one top quark partner undergoes the $\mathrm{T} \to \mathrm{tH}$ decay chain, and the Higgs boson decays to two photons is presented. In order to maximize acceptance and sensitivity to such a small signal, we devise two different sets of event selection criteria, optimized for decay chains with two photons and either no charged leptons or at least one charged lepton. An analysis of 19.7 fb^{-1} of 8 TeV pp collisions reveals no significant excess over background-only predictions. We set an observed (expected) 95% confidence level upper limit on the $\mathrm{T\bar{T}}$ production cross section under several assumptions for the top partner decay chains. Under the hypothesis that $\mathcal{B}(\mathrm{T} \to \mathrm{tH}) = 100\%$, we observe (expect) the exclusion of top quark partners up to $m_{\mathrm{T}} = 540\ (607)$ GeV.

REFERENCES

[1] Chatrchyan S. *et al.*, *Phys. Lett. B*, **716** (2012) 30.
[2] Aad G. *et al.*, *Phys. Lett. B*, **716** (2012) 1.
[3] De Simone A., Matsedonskyi O., Rattazzi R. and Wulzer A., *JHEP*, **1304** (2013) 004.
[4] CMS Collaboration, CMS Physics Analysis Summary B2G-14-003 (2014), https://cds.cern.ch/record/1709129.
[5] Arkani-Hamed N., Cohen A. G. and Georgi H., *Phys. Lett. B*, **513** (2001) 232.
[6] Contino R., Da Rold L. and Pomarol A., *Phys. Rev. D*, **75** (2007) 055014.
[7] Aguilar-Saavedra J., Benbrik R., Heinemeyer S. and Perez-Victoria M., *Phys. Rev. D*, **88** (2013) 094010.
[8] Chatrchyan S. *et al.*, *Phys. Lett. B*, **716** (2012) 103.
[9] Aad G. *et al.*, *Phys. Lett. B*, **718** (2013) 1284.
[10] CMS Collaboration, CMS Physics Analysis Summary CMS-PAS-LUM-13-001 (2013).
[11] CMS Collaboration, CMS Physics Analysis Summary CMS-PAS-HIG-13-001 (2013), http://cds.cern.ch/record/1530524.
[12] Chatrchyan S. *et al.*, *JINST*, **3** (2008) S08004.
[13] Cacciari M., Salam G. P. and Soyez G., *Eur. Phys. J. C*, **72** (2012) 1896.
[14] Cacciari M., Salam G. P. and Soyez G., *JHEP*, **04** (2008) 063.
[15] CMS Collaboration, CMS Physics Analysis Summary CMS-PAS-JME-13-005 (2013), http://cdsweb.cern.ch/record/1581583.
[16] CMS Collaboration, *JINST*, **8** (2013) P04013.
[17] Chatrchyan S. *et al.*, *JINST*, **7** (2012) P10002.
[18] CMS Collaboration, CMS Physics Analysis Summary CMS-PAS-EGM-10-004 (2010), http://cdsweb.cern.ch/record/1299116.
[19] Alwall J., Herquet M., Maltoni F., Mattelaer O. and Stelzer T., *JHEP*, **1106** (2011) 128.
[20] Sjostrand T., Mrenna S. and Skands P. Z., *JHEP*, **0605** (2006) 026.
[21] Czakon M. and Mitov A., arXiv (2011).
[22] Martin A., Stirling W., Thorne R. and Watt G., *Eur. Phys. J. C*, **63** (2009) 189.
[23] Read A., Tech. Rep. CERN CERN-OPEN-2000-005 (2000), http://cdsweb.cern.ch/record/451614.
[24] Junk T., *Nucl. Instrum. Meth. A*, **434** (1999) 435.
[25] ATLAS and CMS Collaborations, LHC Higgs Combination Group, ATL-PHYS-PUB/CMS NOTE 2011-11, 2011/005 (2011), http://cdsweb.cern.ch/record/1379837.